The Journal of
Experimental Biology

RESEARCH ARTICLE

Flexural stiffness and composition of the batoid propterygium as predictors of punting ability

Laura J. Macesic[1],* and Adam P. Summers[2]

[1]Mount Holyoke College, South Hadley, MA 01075, USA and [2]Friday Harbor Laboratories, University of Washington, Friday Harbor, WA 98250, USA

*Author for correspondence (ljmacesic@gmail.com)

SUMMARY

Elasmobranchs (sharks, skates and rays) perform at the extremes of locomotion and feeding (i.e. long migrations, high-speed swimming and durophagy). However, very little is known about their cartilaginous skeletal structure and composition in response to loading regimes. In this study, we investigated a batoid (skate and ray) appendicular skeletal element, the propterygium, and its response to forces experienced during punting (benthic pelvic fin locomotion). Punting places a flexural load on this thin, rod-like element. The goals for our study were to determine: (1) the mechanical and compositional properties of the propterygium and (2) whether these properties correlate with punting ability. Using five batoid species of varying punting ability, we employed a three-point bending test and found that propterygium flexural stiffness (33.74–180.16 Nm^2) was similar to values found in bone and could predict punting ability. Variation in flexural stiffness resulted from differences in mineral content (24.4–48.9% dry mass) and the second moment of area. Propterygia material stiffness (140–2533 MPa) approached the lower limit of bone despite having less than one-third of its mineral content. This drastically lower mineral content is reflected in the radius-to-thickness ratio of the cross-section (mean ± s.e.m.=5.5±0.44), which is comparatively much higher than bony vertebrates. This indicates that elasmobranchs may have evolved skeletal elements that increase buoyancy without sacrificing mechanical properties. Our results highlight the functional parallels between a cartilaginous and bony skeleton despite dramatic compositional differences, and provide insight into how environmental factors may affect cartilaginous skeletal development.

Key words: elasmobranch, material property, cartilage, locomotion.

INTRODUCTION

Depending on the relative proportions of ground substance, collagen and elastin, the function of mammalian cartilage can vary widely: from acting as deformation-resisting shock absorbers between vertebrae to forming highly flexible and elastic structural support for the ears and nose. In contrast, bone must remain stiff to provide support for the body and comprise essential lever systems. However, in the elasmobranchs (sharks, skates and rays), cartilage must perform the functions otherwise carried out by bone, as well as many of the typical functions of cartilage found in bony vertebrates. The elasmobranch cartilaginous skeleton does not appear to limit behaviour, as sharks and batoids (skates and rays) perform extreme durophagy (Huber et al., 2005), carry out long migrations (Bonfil et al., 2005) and are some of the fastest fish in the oceans (Last and Stevens, 1994). Therefore, elasmobranch cartilage must achieve high levels of flexural stiffness in order to resist bending under the high and/or repetitive forces commonly encountered during feeding and swimming (Huber et al., 2005; Gemballa et al., 2006; Martinez et al., 2002). In bony vertebrates, such forces upon the skeleton are met with both proximal and ultimate adaptations aimed at increasing the flexural stiffness (ability to resist bending) and strength (ability to resist fracture) of the bone, including: a thickening of cortical bone (Globus et al., 1984; Woo et al., 1981), an increase in the second moments of area in the axis of loading (Woo et al., 1981), the development of struts within the trabecular bone (Biewener et al., 1996; Carlson et al., 2008) and an increase in mineral content

(Currey, 1969; Dumont, 2010; Kumasaka et al., 2005; Miller et al., 2007; Schaffler and Burr, 1988; Zioupos et al., 1997). The high metabolic activity of bone allows for osteoblasts and osteoclasts to carry out such remodeling by continuously laying down and removing bone tissue, respectively (Currey, 2002). In contrast, very little is known about how the elasmobranch cartilaginous skeleton, which has very low metabolic activity and appears to lack cells for remodeling (Dean et al., 2009), adapts to similar biological loads either on an ontogenetic or an evolutionary time scale.

Elasmobranch cartilage exists in two structural forms: areolar (in the vertebrae) and tessellated (in the cranial and appendicular skeletal elements) (Moss, 1977; Dean and Summers, 2006). Areolar cartilage is a relatively dense, calcified tissue that behaves similarly to mammalian trabecular bone in terms of material stiffness and ultimate strength (Porter et al., 2006). Material stiffness increases with mineralization and can be a good predictor of swimming speed (Porter et al., 2006), which is an indication that the skeletal system may respond to load over evolutionary time. Recent studies (Summers, 2000; Summers et al., 2004) have also demonstrated adaptations of tessellated cartilage in high-stress environments. Tessellated cartilage is composed of an outer layer mosaic of hydroxyapatite tiles, termed tesserae (hundreds of microns deep and wide in adults), which are joined together by intertesseral collagen fibers (Applegate, 1967; Clement, 1992; Dean and Summers, 2006; Kemp and Westrin, 1979). This tiled layer surrounds a core of unmineralized gel, not unlike mammalian hyaline cartilage,
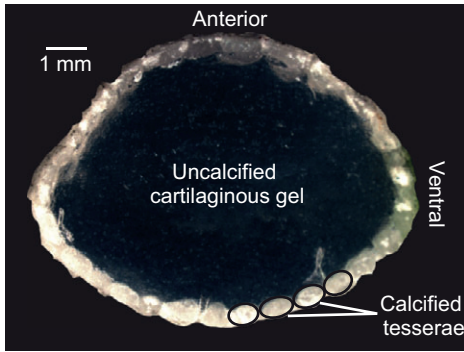
Fig. 1. This cross-sectional slice (anterior side upper, ventral side right) through the propterygium of *Raja eglanteria* shows the outer ring of calcified tesserae (outlined in the lower right of the figure) surrounding the uncalcified cartilaginous gel of the interior.

composed of water and proteoglycan in a matrix of collagen fibers (Dean et al., 2008; Dean et al., 2009) (Fig. 1). In durophagous elasmobranchs, the jaws, which bear very large loads, are composed of multiple layers of tessellated cartilage, arranged to maximize the second moment of area with respect to crushing loads (Summers, 2000; Summers et al., 2004). Dingerkus et al. (Dingerkus et al., 1991) demonstrated that the jaws of large sharks such as the tiger shark, *Galeocerdo cuvieri*, and the great white shark, *Carcharadon carcharias*, also possess multiple layers of tesserae. The number of layers increases only as the sharks, and therefore their prey and the resultant forces experienced during feeding, grow (Dingerkus et al., 1991). Elasmobranch skeletal elements can also exhibit internal trabeculation, as seen in the jaws of durophagous cownose rays, to increase structural stiffness (Summers et al., 1998). Aside from this handful of studies, very little is known about the composition and material properties of the elasmobranch skeleton, and there are no data on these properties for the appendicular skeletal elements.

This study aims to investigate the material and structural properties of a stylopodial element of the appendicular skeleton, the propterygium, across a range of functions. Some batoids use the propterygium, located in the anterior-most portion of the pelvic fin

(Fig. 2), as the main locomotory element during a benthic type of locomotion termed 'punting' (Koester and Spirito, 2003; Lucifora and Vassallo, 2002; Macesic and Kajiura, 2010). Punting is a bilateral, synchronized movement of the pelvic fins in which the anterior lobe of the fin is protracted cranially, planted into the substrate and then retracted caudally to thrust the batoid forward. The batoid then glides and recovers the pelvic fins to prepare for the next cycle. Punting may be performed with the rest of the body remaining motionless, termed true punting (Koester, 2003; Lucifora and Vassallo, 2002; Macesic and Kajiura, 2010), or with additional movement of the pectoral fins, termed augmented punting (Macesic and Kajiura, 2010). Despite the addition of pectoral fin movement, augmented punters have not demonstrated a locomotory advantage, as kinematic variables (e.g. speed, distance travelled per punt and duty factor) do not differ from those of true punters (Macesic and Kajiura, 2010). This suggests that true punters are able to generate locomotor forces with only their pelvic fins that are comparable to forces generated with the combined pectoral and pelvic fins of the augmented punters.

In this study, we examined a phylogenetically diverse group of batoids that includes true punters, augmented punters and a non-punter (Fig. 2). The goals for this study were to determine: (1) the mechanical properties (flexural stiffness, material stiffness and second moment of area) and compositional properties (mineral and water content) of an element of the appendicular skeleton – the propterygium – and (2) whether these apparent mechanical and compositional properties correlate with punting ability and/or phylogeny. This work will not only increase our basic understanding of the mechanical limitations of the elasmobranch skeleton, but will also provide insight into elasmobranch skeletal adaptations to small loads, as previous work has solely focused on responses to relatively large loads.

MATERIALS AND METHODS
Specimens
Five batoid species were used in this study (Fig. 2). Two are true punters: the lesser electric ray [*Narcine bancroftii* (Griffith 1834); Narcinidae; $N=6$, mean ± s.d. disc length (DL)=15.8±2.60cm] and the clearnose skate (*Raja eglanteria* Bosc 1800; Rajidae; $N=6$, DL=21.4±4.31cm); two are augmented punters: the yellow stingray

Fig. 2. The batoids used in this study are true punters, augmented punters and a non-punter. Below each photo, a skeletal schematic of the pelvic fins illustrates the location of the propterygia (red) and the location of the cross-sectional slice. A representative cross-section through each propterygium is also shown.

[*Urobatis jamaicensis* (Cuvier 1816); Urobatidae; *N*=5, DL=18.8±1.52 cm] and the Atlantic stingray [*Dasyatis sabina* (Leseur 1824); Dasyatidae; *N*=6, DL=24.8±3.03 cm]; and one is a non-punter: the pelagic stingray [*Pteroplatytrygon violacea* (Bonaparte 1832); Dasyatidae; *N*=5, DL=39.4±3.63 cm] (Fig. 2). All propterygia were obtained from previously frozen (up to 1 yr) whole-animal specimens. It has been shown that freezing does not affect stiffness properties of vertebrate skeletal tissues, including both uncalcified and calcified elements, such as mammalian articular cartilage (Szarko et al., 2010), mammalian bone and tendon (Jung et al., 2011; Sedlin, 1965), or mammalian dentin (Deymier-Black et al., 2011); however, no data are available for elasmobranch cartilage.

Flexural stiffness

The left and right propterygia from each individual batoid were dissected out of the whole animal and cleaned of muscle and connective tissue. Each propterygium was kept in an individual vial filled with elasmobranch Ringer's solution (Forster et al., 1972) at 6°C for a maximum of 24 h prior to material testing. The total length of the propterygium was measured with a ruler (to the nearest 1 mm), and half of the total length was marked using a felt-tip marker.

Methods for the three-point bending experiment followed those by Horton and Summers (Horton and Summers, 2009). A Synergie 100 test system (MTS, Eden Prairie, MN, USA) with a 500 N load cell was used to perform three-point bending tests to measure flexural stiffness of the entire composite structure (calcified tesserae and uncalcified gelatinous core). The propterygia were supported and tested in a custom-made steel and aluminum fixture mounted in the test system (Fig. 3). Two bottom points, with a 1.2 cm span, supported the propterygium, and one top load point, the indenter, centrally loaded the propterygium. Previous kinematic analysis reveals that the entire skeletal element is in contact with the substrate when punting, thus making a central loading test biologically relevant (Macesic and Kajiura, 2010). Prior to testing, each propterygium was minimally loaded (approximately 0.005 N) to secure it in place and to ensure that there was no rotation along the long axis. Each propterygium was positioned such that the force from the indenter was delivered in the same plane that ground reaction forces would exert during punting. This is mainly on the ventral surface of the skeletal element (Macesic and Kajiura, 2010). The two support load points were in contact with the dorsal surface. Each propterygium was centrally loaded five times, to a maximum deflection of 0.5 mm at a constant test speed (0.5 mm s^{-1}) to mimic the kinematics observed during a typical punting cycle (Macesic and Kajiura, 2010); data were acquired at 120 Hz. There was a rest period in between each of the five loading cycles. To ensure that there was no effect from repeated loading, we performed bending tests with 15 s, 30 s, 1 min and 2 min rest intervals on a propterygium not used in this study. A 1 min rest interval was chosen, as no change in stiffness was observed when using this interval. Elasmobranch Ringer's solution was applied to the propterygium as necessary to prevent desiccation. Each propterygium was then returned to its vial containing elasmobranch Ringer's solution at 6°C for a maximum of 24 h.

Propterygium morphology

Following the three-point bending tests, propterygia were removed from the elasmobranch Ringer's solution, towel dried and color-coded on the ventral and anterior surfaces with felt-tip markers to ensure correct orientation. A microtome blade was used to section a thin cross-sectional slice (~1 mm) at the point of load contact for
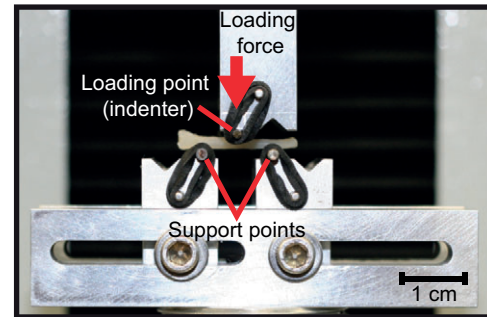

Fig. 3. A propterygium from *R. eglanteria* is positioned in the custom-fit three-point bending rig with the ventral surface in contact with the central loading point (the indenter), and the anterior surface facing the reader. Support points on the lower of the rig were separated by 1.2 cm.

each propterygium. Slices were then digitally photographed using a Zeiss dissecting scope (Stemi 2000-C, Jena, Germany) with a top-mounted Spot Insight color camera (IN-320, Sterling Heights, MI, USA). A scale bar was digitally inserted with the software Axio Scope (Zeiss). Each propterygium was replaced into its vial containing elasmobranch Ringer's solution at 6°C. The software ImageJ (National Institutes of Health, Bethesda, MD, USA) was used to measure tesserae thickness (an average of the anterior, posterior, ventral and dorsal sides) and the cross-sectional area (CSA; mm^2). Because modeling has determined that the stiffness of the element is largely attributed to the tesserae (Liu et al., 2010), only the outer calcified tesserae were included in the CSA (Fig. 3). Additionally, we calculated a radius-to-thickness ratio (*R/t*) of the tesserae (in the dorso-ventral plane, where *R* is the radius of the propterygium cross-section and *t* is the thickness of the tesserae) to gain a better understanding of the effect of wall thickness on the structural properties of the propterygia.

A customized MATLAB (v. 7.0) script (Summers et al., 2004) was used to calculate the second moment of area (*I*; mm^4) with respect to a neutral axis through the center of area parallel to the major axis of the ellipse that best fitted the outline of the cross-section. The following equation was used in the script:

$$I = \int x^2 dA,\qquad(1)$$

where *x* is the distance between the infinitesimal area *dA* and the neutral axis (Beer and Johnston, 1977; Summers et al., 2004; Wainwright et al., 1976). In the three-point bending test, the force was centrally loaded onto the ventral surface of the propterygium; therefore, the neutral axis would be perpendicular to both the long axis of the propterygium and the direction of deflection. Flexural stiffness (*EI*; Nmm^2) was determined using the same script with the beam equation (Beer and Johnston, 1977; Vogel, 2003):

$$EI = \frac{\mathbf{F}l^3}{48 y_{max}},\qquad(2)$$

where y_{max} is the deflection distance of the propterygium, **F** is the force required to deflect the propterygium to the distance of y_{max} (both values obtained in three-point bending tests) and *l* is the span (distance between supports). Using previously calculated values for *I*, we were then also able to calculate apparent material stiffness, *E* (N mm^{-2} or MPa), for the entire composite structure. This is a size and shape independent measure of the stiffness of material alone. By using this beam equation (Eqn 2) to determine *E*, we are assuming that the deformations are caused by bending, and not by

shear, which is generally true for beams with aspect ratios greater than 15 (Spatz et al., 1996). The aspect ratios for the propterygia in this study ranged from eight to 27. However, the values of E for the low aspect ratio propterygia are likely reasonable, as Schriefer et al. (Schriefer et al., 2005) have since found that three-point bending tests resulted in only a 5% error due to shear in mouse bones with aspect ratios of eight. This error value decreased as the aspect ratio increased (Schriefer et al., 2005).

To obtain a dimensionless comparison of I among species, we calculated the ratio of the second moment of the propterygium (I_p) to that of a hollow circle (I_h) with the same area as the mineralized portion of the propterygium cross-section (Summers et al., 2004). To generate values of area for the hypothetical hollow circle, we determined an outer radius (r_o) from each propterygium's CSA that would generate a circular shape, using the equation:

$$r_o = \sqrt{\frac{A_p}{\pi}} \, , \qquad (3)$$

where A_p is the CSA of the propterygium. The inner radius (r_i) was calculated by subtracting the average tesserae thickness from r_o. The I of a hollow circular object of equal radius (I_h) was then calculated using (Vogel, 2003):

$$I_h = \frac{\pi(r_o - r_i)}{4} \, . \qquad (4)$$

Finally, we determined how propterygium flexural stiffness might translate into whole-body kinematic differences during underwater punting. Using the experimentally obtained values for EI, we calculated hypothetical values for the deflection of a propterygium (as a uniformly loaded cantilever beam) when experiencing just the underwater load of body mass for all species at a standardized DL using (Vogel, 2003):

$$y_{max} = \frac{\mathbf{F}l^3}{8EI} \, , \qquad (5)$$

where y_{max} is the maximum displacement of the propterygium, $\mathbf{F}$ is the load of half of the body mass for each species and l is the length of each species' propterygium, as interpolated from the experimental data. From kinematic observations (Macesic and Kajiura, 2010; Koester and Spirito, 2003; Lucifora and Vassallo, 2002), it appears that the entire propterygium is making contact with the substrate; therefore, the equation for the uniformly loaded cantilever beam was used. We chose a DL of 20 cm because it is a size that all five species in this study reach as adults (Bigelow and Schroeder, 1953; Compagno, 1999). The body mass was halved to estimate the load experienced by each propterygium during a punt when both fins are employed simultaneously. Masses of animals were obtained from previously published reports for these species. To simulate the force of each animal's mass underwater, we used the underwater mass [2% of the land mass (Bone and Roberts, 1969)]. Bending moments (M; Nmm) experienced by each propterygia for a batoid of 20 cm DL were calculated as the product of each species' estimated underwater mass and the length of the propterygium. Wingspan can vary widely among species, and masses of each individual used in this study were not all available for further interpolation; therefore, we used DL as a reliable estimator of body size.

Composition

Upon completion of the mechanical testing, the pieces of each propterygium were analyzed for mineral and water content. The propterygia were towel-dried and individually massed to obtain the
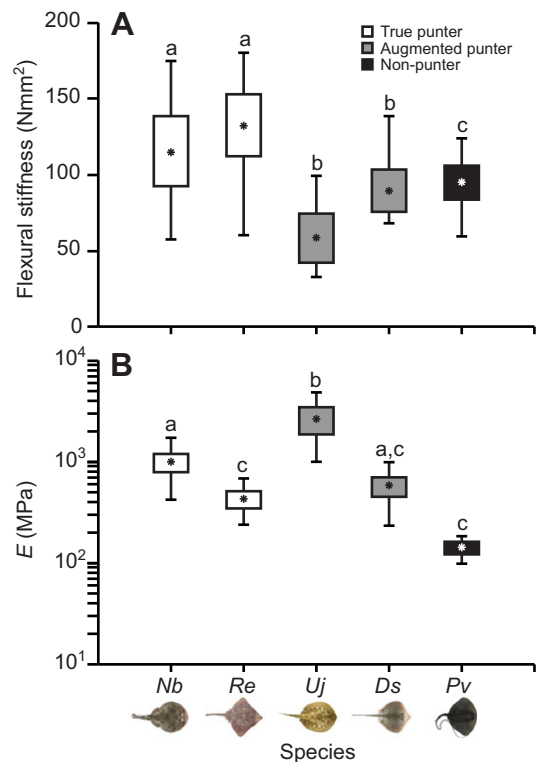

Fig. 4. Box-and-whisker plot of the mechanical properties of the propterygium showing variation among species and punting ability. Boxes represent the 95% confidence intervals, asterisks represent means and whiskers represent the maximum and minimum values. Species that are not statistically different from each other share a common letter. Flexural stiffness (A) demonstrated obvious trends with punting ability; however, variation in material stiffness (B) did not follow this same trend. True punters are depicted in white; augmented punters are depicted in gray; the non-punter is depicted in black. *Nb*, *Narcine bancroftii*; *Re*, *Raja eglanteria*; *Uj*, *Urobatis jamaicensis*; *Ds*, *Dasyatis sabina*; *Pv*, *Pteroplatytrygon violacea*.

wet mass. They were then lyophilized at 90°C for 24 h and reweighed to obtain the dry mass (organic and mineral content). The propterygia were ashed in a muffle furnace for another 24 h at 450°C, and immediately reweighed to obtain the ash-free dry mass (mineral content). Water content was calculated by subtracting the dry mass from the wet mass and dividing this by the total wet mass. Organic content was calculated by subtracting the ash-free dry mass and the water mass from the total wet mass and dividing this by the total wet mass. Mineral content was also expressed as a proportion of the dry mass by dividing the ash-free dry mass by the total dry mass.

Statistical analyses

Data were analyzed in SPSS (v. 18.0, IBM, Armonk, NY, USA). The mean values for the five three-point bending tests for each left and right propterygia were used in the statistical analyses for flexural stiffness, material stiffness and second moment of area. Paired t-tests were performed to determine differences between the left and right propterygia for all variables. No differences were found ($P > 0.05$ for all); therefore, the two sides were pooled and one average value for each individual (combining left and right sides) was used to determine differences among species for each variable ($N=5$ for *U. jamaicensis* and *P. violacea*; $N=6$ for *N. bancroftii*, *R. eglanteria* and *D. sabina*). We used an analysis of covariance
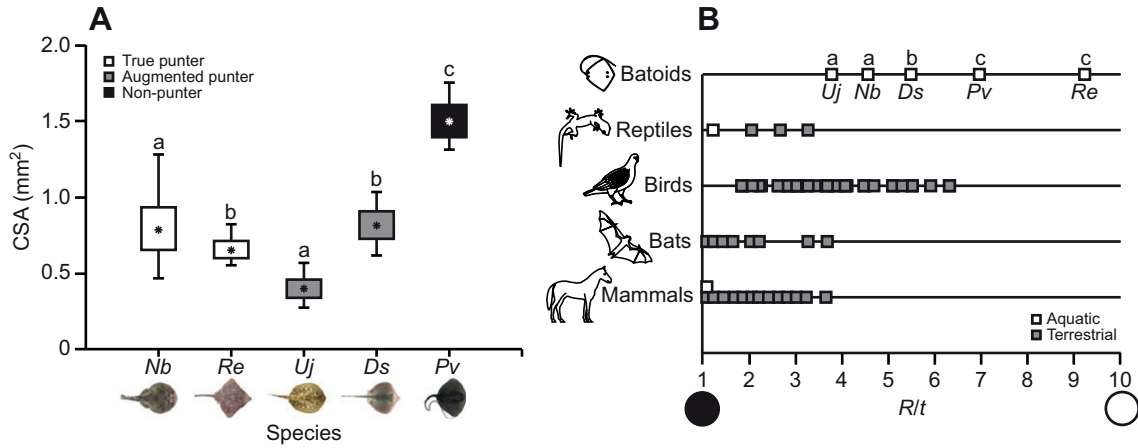
Fig. 5. Amount and distribution of calcified material in the propterygium, normalized to body size. (A) The box-and-whisker plot of the cross-sectional area of tesserae. Boxes represent the 95% confidence intervals, asterisks represent means and whiskers represent the maximum and minimum values. CSA varies among species but does not correlate to punting ability. True punters are depicted in white; augmented punters are depicted in gray; the non-punter is depicted in black. *Nb*, *Narcine bancroftii*; *Re*, *Raja eglanteria*; *Uj*, *Urobatis jamaicensis*; *Ds*, *Dasyatis sabina*; *Pv*, *Pteroplatytrygon violacea*. (B) Values of *R/t* (cross-sectional radius/outer-wall thickness) for various vertebrates, including data from this study on the propterygia of batoids. Terrestrial vertebrates are shown in gray squares, aquatic vertebrates in white squares. Representative cross-sections with *R/t* values of 1 and 10 are depicted on the bottom left and right of the figure, respectively. Among batoids, *R/t* values are significantly highest in the pelagic stingray (*Dv*) and the clearnose skate (*Re*), and lowest in the lesser electric ray (*Nb*) and the yellow stingray (*Uj*). Species that are not statistically different from each other share a common letter. Comparative data are from Currey and Alexander (Currey and Alexander, 1985) and Currey (Currey, 2002).

(ANCOVA) with disc length as the covariate to determine differences among the species in: propterygium length, tesserae thickness, second moment of area, flexural stiffness, material stiffness, CSA, radius to tesserae thickness ratio (*R/t*), mineral content and water content. This allowed us to remove size effects among the species. Mineral content and water content from all of the species were pooled and regressed and fit with a best-fit line against flexural stiffness and against material stiffness to determine the content contributions to these mechanical properties. We performed an ANOVA on the ratios of I_p:I_h to determine differences among species. We performed *post hoc* analyses using the Tukey–Kramer method for comparison among unequal sample sizes. In order to achieve normality and homoscedasticity, we log-transformed I and R/t prior to analyses. Data are presented as means ± s.e.m. unless otherwise indicated.

RESULTS

Mean flexural stiffness (*EI*) of the propterygium ranged from 33.7 to 180.2 Nmm^2 and varied significantly among species (ANCOVA: $F_{4,22}$=15.99, *P*<0.01; Fig. 4A). Relative to their size, the true punting *R. eglanteria* had propterygia with the greatest flexural stiffness (126.1±16.43 Nmm^2; Fig. 4A). Both of the augmented punters, *U. jamaicensis* and *D. sabina*, possess propterygia with less flexural stiffness than the true punters (56.14±10.57 and 89.4±10.03 Nmm^2, respectively; Tukey–Kramer, *P*<0.05), but greater than the non-punter, *P. violacea* (94.9±7.49 Nmm^2; Tukey–Kramer, *P*<0.05; Fig. 4A). Material stiffness (*E*) also differed significantly among species (ANCOVA: $F_{4,18}$=3.86, *P*<0.05; Fig. 4B). *Urobatis jamaicensis* had propterygia with the greatest material stiffness (2.54×10^3 ±3.9×10^2 MPa; Tukey–Kramer, *P*<0.05), and the two dasyatids, *D. sabina* (5.40×10^2±6.4×10 MPa; Tukey–Kramer, *P*<0.05) and *P. violacea* (1.40×10^2±1.3×10 MPa; Tukey–Kramer, *P*<0.05), possessed the propterygia with the least material stiffness (Fig. 4B). The propterygia of *N. bancroftii* and *R. eglanteria* exhibited intermediate values for material stiffness (9.89×10^2±1.4×10^2 and 4.09×10^2±5.8×10 MPa, respectively).

Propterygium morphology

Propterygia length varied among the species (ANCOVA: $F_{4,18}$=19.914, *P*<0.01): the true punters *R. eglanteria* and *N. bancroftii* possess significantly longer propterygia than the augmented punters and non-punters (Tukey–Kramer, *P*<0.01). Because these and other data are normalized for body size, differences reflect true variation among species when at a standardized body size, and not variation as an ontogenetic artifact. There was less variation in the thickness of the propterygium's calcified outer layer of tiled tesserae. The tesserae of *N. bancroftii* (0.21±0.042 mm) were significantly thicker than the tesserae of the other species (compiled mean=0.14±0.015 mm, ANCOVA, *P*<0.05 for all). We found that the CSA of each propterygium at the midpoint also varied among species (ANCOVA: $F_{4,22}$=14.178, *P*<0.01; Fig. 5A). *Pteroplatytrygon violacea* had propterygia with the largest CSA (6.72±0.344 mm^2; Tukey–Kramer, *P*<0.01), whereas *U. jamaicensis* had propterygia with the smallest CSA (0.87±0.070 mm^2; Tukey–Kramer, *P*<0.01; Fig. 5A). The *R/t* ratio was variable among the species (ANCOVA: $F_{4,22}$=54.469, *P*<0.01; Fig. 5B), with the greatest *R/t* ratio seen in *R. eglanteria* (9.0±0.33) and *P. violacea* (7.1±0.80), and the lowest seen in *U. jamaicensis* (2.8±0.41) and *N. bancroftii* (3.5±0.47). Overall, despite differences in CSA, tesserae thickness did not exhibit much variability, contributing to greater differences in *R/t*.

The second moment of area (*I*) differed significantly among species (ANCOVA: $F_{4,22}$=49.488, *P*<0.01; Fig. 6A). As shown in Fig. 6A, *I* was greatest in the propterygia of *P. violacea* and *R. eglanteria* (Tukey–Kramer, *P*<0.01; Fig. 6A), followed by that of *N. bancroftii* and *D. sabina* (Tukey–Kramer, *P*<0.01; Fig. 6A). The ratio of I_p:I_h also varied among species (ANOVA: $F_{4,22}$=87.99, *P*<0.01; Fig. 6B); however, this ratio was greatest in the true punter *R. eglanteria* (1.34±0.046; Tukey–Kramer, *P*<0.05). Whereas the ratios for two true punters approximate or were greater than one, the ratios for the augmented punters and non-punter were considerably less than one (Fig. 6B). Ratio values ranged between 0.55±0.028 in *U. jamaicensis* and 0.62±0.021 in *P. violacea* (Fig. 6B). The I_p:I_h values of the augmented punters and the non-
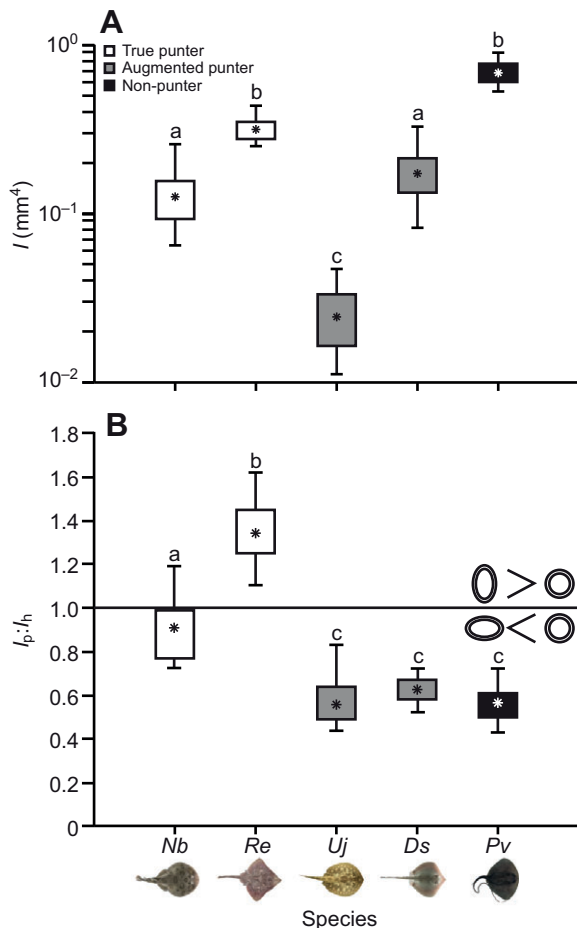
Fig. 6. Box-and-whisker plots of (A) the second moment of area and (B) a comparative shape analysis of the calcified material in the propterygia. Boxes represent 95% confidence intervals, asterisks represent means and whiskers represent the maximum and minimum values. (A) The absolute values of the second moment of area differ among species but do not reflect the punting mode. (B) The ratio of the second moment of area of the propterygium to the second moment of area of a hollow circular object with equal cross-sectional area (I_p:I_h) illustrates the shape differences among the species by removing the effects of size. Values greater than one indicate that the propterygia are better than a hollow circular object at resisting bending. The I_p:I_h ratio is the greatest in the true punters *R. eglanteria* and then *N. bancroftii*. Ratios for both species demonstrate similar or greater ability than a hollow circular rod at resisting bending. In contrast, the ratios of the augmented and non-punters do not differ from each other and are lower than one. *Nb*, *Narcine bancroftii*; *Re*, *Raja eglanteria*; *Uj*, *Urobatis jamaicensis*; *Ds*, *Dasyatis sabina*; *Pv*, *Pteroplatytrygon violacea*.

punter were not significantly different from each other (Tukey–Kramer, $P>0.05$).

Composition

The mineral content of the propterygia varied among species (ANCOVA: $F_{4,22}$=10.21, $P<0.01$; Fig. 7A, lower half), with values ranging from 24.40% of the dry mass in *P. violacea* to 48.94% in *N. bancroftii*. The propterygia of *N. bancroftii* and *U. jamaicensis* did not differ significantly in terms of mineral content (Tukey–Kramer, $P=0.23$; Fig. 7A, lower half), and they possessed the greatest percentage of mineral content overall (Tukey–Kramer, $P<0.01$; Fig. 7A, lower half). The mineral content of *P. violacea*'s propterygia was significantly lower than that of the other batoids

(Tukey–Kramer, $P<0.01$; Fig. 7A, lower half). The pooled values for mineral content across the species were not significantly correlated with *EI* (R^2=0.001, P=0.90); however, there was a positive logarithmic relationship between mineral content and material stiffness [y=4.94ln(x)+6.21, R^2=0.68, $P<0.01$; Fig. 7B, black squares, solid line].

The water content of the propterygia varied among species (ANCOVA: $F_{4,22}$=6.397, $P<0.01$; Fig. 7A, upper half). The propterygia of *N. bancroftii* and *U. jamaicensis* contained significantly less water than those of the other species (Tukey–Kramer, $P<0.01$; Fig. 7A, upper half). In contrast, the propterygia of *P. violacea* contained significantly more water than those of the other batoids (80.97±0.360%; Tukey–Kramer, $P<0.01$; Fig. 7A, upper half). Water content was not significantly correlated with *EI* (R^2=0.165, P=0.21); however, there was a negative logarithmic relationship between water content and material stiffness [y=–3.81ln(x)+97.53, R^2=0.63, $P<0.01$; Fig. 7B, white squares, dashed line]. In general, the total volume of the batoid propterygium was dominated by water (73.3±8.77%), followed by organic material (16.4±0.36%) and minerals (10.3±0.57%; Fig. 8).

DISCUSSION

We have demonstrated that the flexural stiffness of the batoid propterygium correlates with punting ability, thus providing a clear link between form and function for the appendicular skeletal elements of elasmobranchs. Moreover, despite having an entirely cartilaginous skeleton, the five species of batoids exhibited values of flexural stiffness that are comparable to those of similarly sized bony appendicular bones, such as the bat forelimb [10–1560 Nmm^2 (Swartz and Middleton, 2008; Reilly and Burstein, 1975; Reilly et al., 1974)], yet they achieve these values with considerably less mineral and more water content (Fig. 8). True punters (*N. bancroftii* and *R. eglanteria*) have propterygia with the highest flexural stiffness, the non-punter (*P. violacea*) has propterygia with the lowest flexural stiffness and the augmented punters (*U. jamaicensis* and *D. sabina*) have propterygia that had flexural stiffness values that were higher than those of the non-punter, but lower than those of the true punters. The high flexural stiffness of the propterygium in true punters may lead to a more efficient transfer of the protractor muscle contraction to pelvic fin movement. Conversely, the low flexural stiffness in the non-punting *P. violacea* implies that stiffness is not gained without cost, because it is lost with the loss of locomotor need. Although a broader phylogenetic sampling needs to be investigated, our data suggest that flexural stiffness may not simply follow phylogeny, as the two members of Dasyatidae (*D. sabina* and *P. violacea*) exhibited significantly different levels of flexural stiffness that correlated with punting ability. This is in agreement with previous work by Dingerkus et al. (Dingerkus et al., 1991), which demonstrated that morphological specializations that confer greater stiffness in the jaws of sharks were attributed to ecological performance rather than to phylogenetic patterns. Our study reveals that variation in flexural stiffness can result from changes in shape or composition of the propterygium, suggesting that trade-offs may exist which limit how mechanical properties are achieved.

Depending on the species investigated in this study, flexural stiffness values were driven by material stiffness, cross-sectional shape or both. For example, both the skate *R. eglanteria* and the electric ray *N. bancroftii* have propterygia that exhibit the greatest flexural stiffness, but achieve it in different ways. The skate propterygia have relatively low CSA and material stiffness but a high second moment of area, whereas the electric ray propterygia
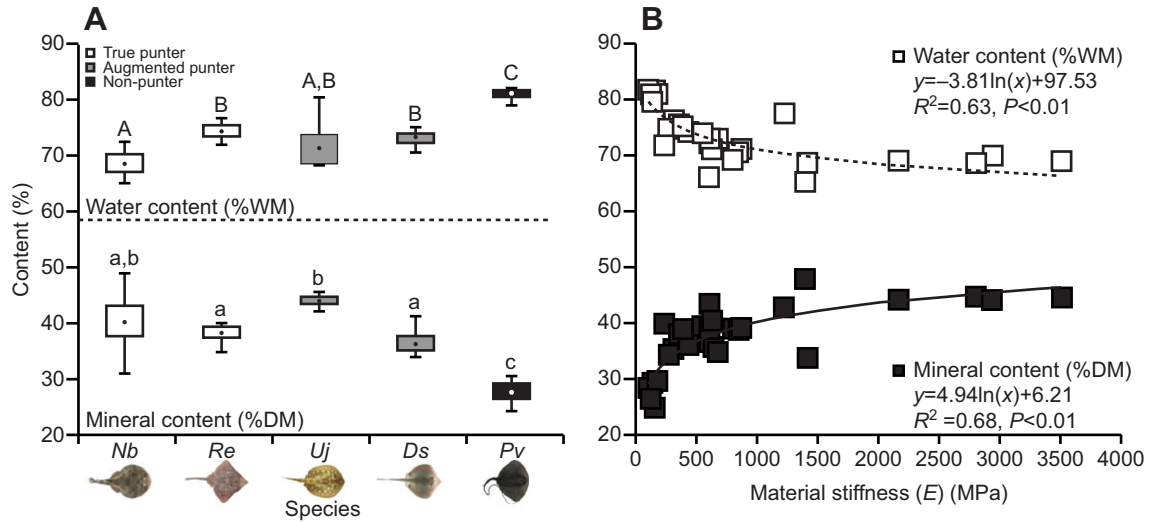
Fig. 7. (A) Box-and-whisker plot of water content [as percent wet mass (WM); upper half of figure, uppercase letters] and mineral content [as percent dry mass (DM); lower half of figure, lowercase letters]. Boxes represent the 95% confidence intervals, asterisks represent means and whiskers represent the maximum and minimum values. Species sharing the same letter are not statistically different from one another. The propterygia of the pelagic stingray, *P. violacea* (*Pv*), have significantly greater water content and less mineral content than all other species. In contrast, the electric ray, *N. bancroftii* (*Nb*), possesses propterygia with the lowest water content and, along with the yellow stingray, *U. jamaicensis* (*Uj*), the greatest mineral content. *Re*, *Raja eglanteria*; *Ds*, *Dasyatis sabina*. (B) For all species combined, water content (white squares) exhibits a significantly negative logarithmic relationship with material stiffness (*E*), whereas mineral content (black squares) exhibits a significantly positive logarithmic relationship with *E*.

have higher CSA and material stiffness, and a lower second moment of area. Similarly, the propterygia of *P. violacea* exhibit the lowest flexural stiffness as a result of having the lowest material stiffness as well as a shape that does not maximize the propterygia's ability to resist bending. These examples demonstrate not only that there is variation in the structural properties that dictate performance, but also that a structural property itself can be modulated in multiple ways.

Although there are no reported values of skeletal flexural stiffness in other elasmobranchs, material stiffness values for shark vertebrae when under compression [322–978 MPa (Porter et al., 2006; Porter et al., 2007)] are within the lower range of values that were found for the appendicular propterygium during bending (140–2533 MPa). However, the only previously reported value of material stiffness in a batoid skeletal element [vertebrae from a basal electric ray, *Torpedo californica* (Porter et al., 2006)] is much lower than this study's values for the closely related *N. bancroftii* (25 and 1300 MPa, respectively). This difference may reflect the functional differences between these two skeletal elements: the propterygia continually experience punting forces, whereas vertebrae are hypothesized to experience very low stresses during axial undulation (Porter et al., 2006). Additionally, this may reflect differences in the compressive *versus* bending loads for which the vertebrae and propterygia were being tested, respectively.

From our study, it is clear that elasmobranch appendicular calcified cartilage is much stiffer than the calcified cartilage that exists in bony mammals prior to bone replacement [350 MPa (Mente and Lewis, 1994)], and instead has values that are similar to the lower range of values for mammalian trabecular bone [800–34,100 Mpa (Currey, 1999; Meyers et al., 2008)]. However, the propterygia have material stiffness values that are well below those for the morphologically similar hollow, long bones of birds (9069–20,980 MPa) (Cubo and Casinos, 2000) (Fig. 9) and bones of teleost fish (Erickson et al., 2002; Horton and Summers, 2009; Roy et al., 2000), including the pelvic metapterygium of bichirs

(*Polypterus* spp.), which are used to swim in water and occasionally foray onto land (Erickson et al., 2002). In these other cartilaginous and bony skeletal elements, mineral content has a positive linear relationship with material stiffness (Currey, 2002). In contrast, though mineral content within the propterygia increases the material stiffness at lower levels, the relationship is logarithmic and material stiffness plateaus at higher levels of mineral content (Fig. 7B). This suggests that there is an upper limit of mineral content that can exist within the tesseral layer. Therefore, despite similar values in
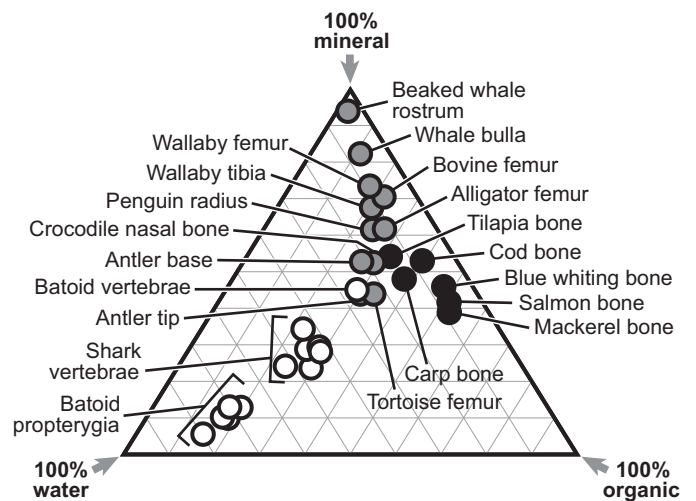

Fig. 8. Ternary diagram of the constituents of various skeletal elements: bone from terrestrial vertebrates (gray circles) and teleost fish (black circles), and calcified cartilage from batoid propterygia (this study) and the vertebral column of elasmobranchs (white circles). Relative proportions were determined by mass. Comparative data are from various sources (Cohen et al., 2012; Currey, 2002; Porter et al., 2006; Toppe et al., 2007; Zioupos et al., 2000).
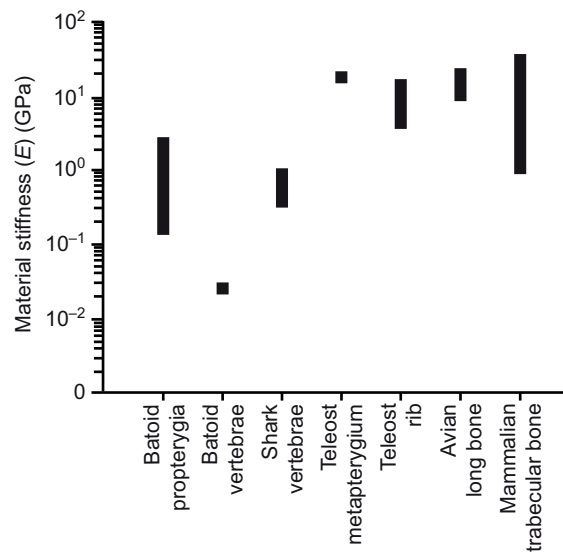
Fig. 9. Comparative values of material stiffness (E) among vertebrates. This study's values for material stiffness of the propterygia overlap previously reported values for elasmobranch vertebral cartilage and the lower limits of bone. Comparative data are from various sources (Cubo and Casinos, 2000; Currey, 2002; Erickson et al., 2002; Horton and Summers, 2009; Porter et al., 2006; Porter et al., 2007; Roy et al., 2000).
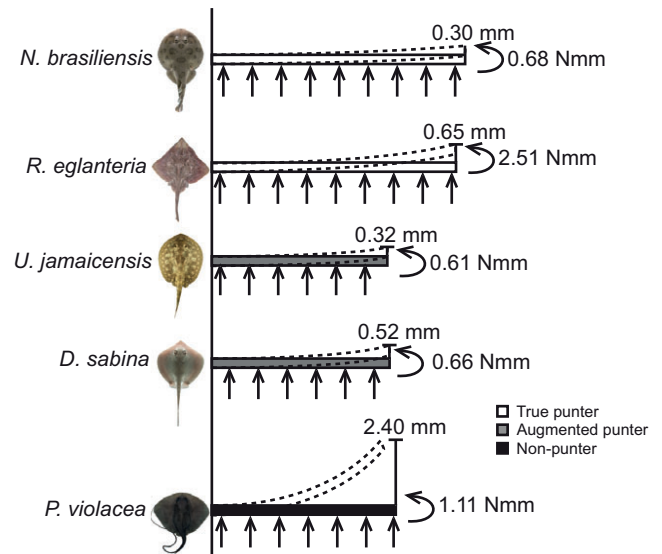

Fig. 10. Theoretical deflection of the propterygia, treated as a uniformly loaded cantilever beam under the force of underwater body mass of a 20 cm disc length (DL) individual. Propterygia lengths for a DL of 20 cm were interpolated from the experimental data. Straight arrows demonstrate the loading of body mass force. Bending moments (Nmm) experienced by each propterygium are given beside the curved arrows. The original position of the propterygium is shown with a solid, horizontal bar; the resultant, bent propterygium is shown with dashed lines. Maximum deflection distance values (mm) are given above each deflected propterygium.

material stiffness, typical mineral volume of long bones from terrestrial vertebrates is closer to 65%, whereas mineral volume of the analogous propterygia is only approximately 10% (Fig. 8). This suggests that the tiled arrangement of the tesserae and/or the large, uncalcified gel core may be significant contributors to the overall material stiffness and, therefore, the flexural stiffness of the elasmobranch appendicular skeletal element.

The ability to achieve values of flexural and material stiffness similar to those of bone but with very little mineral may be an adaptation to achieve requisite mechanical properties without increasing body mass. Neutral or even positive buoyancy can be achieved in bony fish with air-filled gas bladders (Jones, 1957), and in semiaquatic tetrapods (i.e. alligators and penguins) with lungs, but even they tend to possess bones with lower mineral volume, and thus mass, than terrestrial vertebrates (Fig. 8). However, elasmobranchs have denser bodies and no gas bladders or lungs, and thus depend on adaptations such as a lipid-rich liver and the presence of positively buoyant metabolites such as urea and trimethylamine oxide to attain a slightly negative buoyancy (Alexander, 1993; Bone and Roberts, 1969; Withers et al., 1994). The configuration of the appendicular skeleton may be another buoyancy-enhancing adaptation. Data from this study suggest that relatively high levels of material stiffness may be achieved with much lower levels of mineral volume than is seen in other bony vertebrates (Fig. 8). Because an increase in mineral would increase the density of the tesseral layer, buoyancy would be reduced and thus energetic requirements for locomotion would be increased (Alexander, 1993). Interestingly, it has been reported that *N. bancroftii*, which has propterygia with high mineral content and the thickest tesseral layer, is often 'seen lying on bottom', and is 'described as sluggish in habit' compared with other benthic batoids (Bigelow and Schroeder, 1953), whereas the batoid with the lowest mineral content, *P. violacea*, is a pelagic batoid and is thought to perform long migrations (Mollet, 2002).

The reduced mineral content, which is found within the calcified tesseral layer, translates into remarkably high R/t values when compared with other vertebrate bones (Fig. 5B). Such high values can reduce the mass of the element, but also can increase the potential for mechanical failure by buckling (Brazier, 1927). The batoids with the greatest R/t values (*R. eglanteria* and *P. violacea*; Fig. 5B) illustrate that even if CSA and tesseral thickness are equal between two species, the mineral content, and thus density, can significantly differ and affect the material stiffness and thus flexural stiffness of the skeletal element. A similar trend can be observed in avian bones, which are thin-walled and air-filled to reduce mass, yet are very stiff as a result of exceptionally dense bone (Fig. 5B) (Dumont, 2010). In contrast, *U. jamaicensis* and *N. bancroftii* do not exhibit the dramatic difference in density illustrated by *R. eglanteria* and *P. violacea* (Fig. 7A), but instead, although possessing propterygia with similar CSA and R/t values, differ in flexural stiffness as a result of different cross-sectional shapes (Fig. 6B). The propterygia of augmented punters may not experience the loads requisite to develop cross-sectional shapes that maximize the second moment of area because their punts are augmented with pectoral fin movements. The hypothesis that the elasmobranch appendicular skeleton is adapted to increase buoyancy may also explain why the propterygia do not employ multiple layers of tesserae to increase stiffness, as is observed in the tessellated jaws of durophagous elasmobranchs (Summers, 2000; Summers et al., 2004). Although this may be in effort to maintain lightweight fins for locomotion, the loads experienced throughout the appendicular skeleton may not be sufficient to warrant such reinforcements. The fully aquatic batoids can likely afford high R/t values and just a single layer of tesserae, as the ground reaction forces underwater are a fraction of the forces experienced on land and during hard prey processing.

To better illustrate how these values of flexural stiffness can be interpreted during punting, we used *in vitro* data from our mechanical tests to predict propterygium behaviour *in vivo*. For example, we can determine the deflection of each species' propterygia for animals of equal DL (20 cm). Although these predicted values may not be absolute, they do represent the relative behaviors of this set of species. Under normal, synchronous punting conditions, the propterygium of true and augmented punters would minimally deflect (0.30–0.65 mm) under each respective batoid's body mass (Fig. 10). The propterygia of these punting batoids would likely provide sufficient leverage during a punt to generate sufficient ground reaction forces. In contrast, the propterygium of the non-punting *P. violacea* deflects at least four times the distance of the other batoids (2.40 mm; Fig. 10), indicating that it would not be as efficient in generating ground reaction forces necessary to thrust the body up and forward off of the substrate during punting. This example suggests that as the need to punt is lost, so are the structural and material properties of the skeletal element associated with flexural stiffness.

Conclusions

In this study, we demonstrate that the elasmobranch appendicular skeleton has mechanical and morphological properties that are similar to the lower limits of bone. Furthermore, the skeleton reveals the expected load regime even though these loads are quite low in an absolute sense. Future research should be aimed at determining whether these responses to load are a plastic response and whether specific ecological or developmental signals result in these changes. Moreover, research should also focus on *in vivo* experiments to determine the actual strain on the propterygium during punting. The appendicular skeleton of elasmobranchs is achieving levels of flexural and material stiffness that rival those of bone, yet with just a fraction of the mineral volume. Therefore, appendicular skeletal elements from a broad selection of batoids and sharks should be investigated for variation in the composition, size, axis orientation and jointed arrangement of the tiled tesserae as they relate to loading regimes. Additionally, further mechanical studies should be aimed at understanding the interactions between the calcified and uncalcified regions of the skeletal element. This work will increase our understanding of the evolution of this extremely successful, yet understudied, ancient skeletal system.

REFERENCES

Alexander, R. M. (1993). Buoyancy. In *The Physiology of Fishes* (ed. D. H. Evans), pp. 75-97. Boca Raton, FL: CRC Press.

Applegate, S. (1967). A survey of shark hard parts. In *Sharks, Skates and Rays* (ed. P. Gilbert, R. Mathewson and D. Rall), pp. 37-66. Baltimore, MD: Johns Hopkins Press.

Beer, F. P. and Johnston, E. R., Jr (1977). *Vector Mechanics for Engineers: Statics and Dynamics*. New York: McGraw Hill.

Biewener, A. A., Fazzalari, N., Konieczynski, D. and Baudinette, R. (1996). Adaptive changes in trabecular architecture in relation to functional strain patterns and disuse. *Bone* **19**, 1-8.

Bigelow, H. B. and Schroeder, W. C. (1953). Sawfishes, guitarfishes, skates, and rays. In *Fishes of the Western North Atlantic, Part 2: Memoir: Sears Foundation for Marine Research* (ed. J. Tee-Van, C. M. Breeder, A. E. Parr, W. C. Schroeder and L. P. Schultz). pp. 112, 165, 370. New Haven, CT: Yale University Press.

Bone, Q. and Roberts, B. (1969). The density of elasmobranchs. *J. Mar. Biol. Assoc. UK* **49**, 913-937.

Bonfil, R., Meyer, M., Scholl, M. C., Johnson, R., O'Brien, S., Oosthuizen, H., Swanson, S., Kotze, D. and Paterson, M. (2005). Transoceanic migration, spatial dynamics, and population linkages of white sharks. *Nature* **310**, 100-103.

Brazier, L. G. (1927). On the flexure of thin cylindrical shells and other "thin" sections. *Proc. R. Soc. Lond. A* **116**, 104-114.

Carlson, K. J., Lublinsky, S. and Judex, S. (2008). Do different locomotor modes during growth modulate trabecular architecture in the murine hind limb? *Integr. Comp. Biol.* **48**, 385-393.

Clement, J. (1992). Re-examination of the fine structure of endoskeletal mineralization in Chondrichthyes: implications for growth, ageing and calcium homeostasis. *Aust. J. Mar. Freshw. Res.* **43**, 157-181.

Cohen, L., Dean, M., Shipov, A., Atkins, A., Monsonego-Ornan, E. and Shahar, R. (2012). Comparison of structural, architectural and mechanical aspects of cellular and acellular bone in two teleost fish. *J. Exp. Biol.* **215**, 1983-1993.

Compagno, L. J. V. (1999). Checklist of living elasmobranchs. In *Sharks, Skates, and Rays: The Biology of Elasmobranch Fishes* (ed. W. C. Hamlett), pp. 471-498. Baltimore, MD: Johns Hopkins University Press.

Cubo, J. and Casinos, A. (2000). Mechanical properties and chemical composition of avian long bones. *Eur. J. Morphol.* **38**, 112-121.

Currey, J. D. (1969). The mechanical consequences of variation in the mineral content of bone. *J. Biomech.* **2**, 1-11.

Currey, J. D. (1999). What determines the bending strength of compact bone? *J. Exp. Biol.* **202**, 2495-2503.

Currey, J. D. (2002). *Bones*. Princeton, NJ: Princeton University Press.

Currey, J. D. and Alexander, R. M. (1985). The thickness of the walls of tubular bones. *J. Zool.* **206**, 453-468.

Dean, M. N. and Summers, A. P. (2006). Mineralized cartilage in the skeleton of chondrichthyan fishes. *Zoology* **109**, 164-168.

Dean, M. N., Gorb, S. and Summer, A. P. (2008). A cryoSEM method for preservation and visualization of calcified shark cartilage (and other stubborn heterogeneous skeletal tissues). *Microsc. Today* **16**, 48-50.

Dean, M. N., Hale, L. F., Mull, C. G., Gorb, S. N. and Summers, A. P. (2009). Ontogeny of the tessellated skeleton: insight from the skeletal growth of the round stingray, *Urobatis halleri*. *J. Anat.* **215**, 227-239.

Deymier-Black, A. C., Almer, J. D. and Haeffner, D. R. (2011). Effect of freeze–thaw cycles on load transfer between the biomineral and collagen phases of bovine dentin. *Mater. Sci. Eng. C* **31**, 1423-1428.

Dingerkus, G., Séret, B. and Guilbert, E. (1991). Multiple prismatic calcium phosphate layers in the jaws of present-day sharks (Chondrichthyes; Selachii). *Experientia* **47**, 38-40.

Dumont, E. R. (2010). Bone density and the lightweight skeletons of birds. *Proc. R. Soc. Lond. B* **277**, 2193-2198.

Erickson, G. M., Catanese, J. and Keaveny, T. M. (2002). Evolution of the biomechanical material properties of the femur. *Anat. Rec.* **268**, 115-124.

Forster, R. P., Goldstein, L. and Rosen, J. K. (1972). Intrarenal control of urea reabsorption by renal tubules of the marine elasmobranch, *Squalus acanthias*. *Comp. Biochem. Physiol.* **42A**, 3-12.

Gemballa, S., Konstantinidis, P., Donley, J. M., Sepulveda, C. and Shadwick, R. E. (2006). Evolution of high-performance swimming in sharks: transformations of the musculotendinous system from subcarangiform to thunniform swimmers. *J. Morphol.* **267**, 477-493.

Globus, R. K., Bikle, D. D. and Morey-Holton, E. (1984). Effects of simulated weightlessness on bone-mineral metabolism. *Encodrinol.* **114**, 2264-2270.

Horton, J. M. and Summers, A. P. (2009). The material properties of acellular bone in a teleost fish. *J. Exp. Biol.* **212**, 1413-1420.

Huber, D. R., Easton, T. G., Heuter, R. E. and Motta, P. J. (2005). Analysis of the bite force and mechanical design of the feeding mechanism of the durophagous horn shark *Heterodontus francisci*. *J. Exp. Biol.* **208**, 3553-3571.

Jones, F. R. H. (1957). The swimbladder. In *Physiology of Fishes*, Vol. 2 (ed M. E. Brown), pp. 305-322. New York: Academic Press.

Jung, H. J., Vangipuram, G., Fisher, M. B., Yang, G., Hsu, S., Bianchi, J., Ronholdt, C. and Woo, S. L. (2011). The effects of multiple freeze-thaw cycles on the biomechanical properties of the human bone-patellar tendon-bone allograft. *Orthop. Res.* **8**, 1193-1198.

Kemp, N. E. and Westrin, S. K. (1979). Ultrastructure of calcified cartilage in the endoskeletal tesserae of sharks. *J. Morph.* **160**, 75-101.

Koester, D. M. and Spirito, C. P. (2003). Punting: an unusual mode of locomotion in the little skate, *Leucoraja erinacea* (Chondrichthyes: Rajidae). *Copeia* **3**, 553-561.

Kumasaka, S., Asa, K., Kawamata, R., Okada, T., Miyake, M. and Kashima, I. (2005). Relationship between bone mineral density and bone stiffness in bone fracture. *Oral Radiol.* **21**, 38-40.

Last, P. R. and Stephens, J. D. (ed.) (2009). Lamnidae (mackerel sharks). In *Sharks and Rays of Australia*, pp. 174-180. Collingwood, VIC: CSIRO.

Liu, X., Dean, M. N., Summers, A. P. and Earthman, J. C. (2010). Composite model of the shark's skeleton in bending: a novel architecture for biomimetic design of functional compression bias. *Mater. Sci. Eng. C* **30**, 1088-1084.

Lucifora, L. O. and Vassallo, A. I. (2002). Walking in skates (Chondrichthyes, Rajidae): anatomy, behaviour and analogies to tetrapod locomotion. *Biol. J. Linn. Soc.* **77**, 35-41.

Macesic, L. J. and Kajiura, S. M. (2010). Comparative punting kinematics and pelvic fin musculature of benthic batoids. *J. Morphol.* **271**, 1219-1228.

Martinez, G., Drucker, E. G. and Summers, A. P. (2002). Under pressure to swim fast. *Integr. Comp. Biol.* **42**, 1273-1274.

Mente, P. L. and Lewis, J. L. (1994). Elastic modulus of calcified cartilage is an order of magnitude less than that of subchondral bone. *J. Orthop. Res.* **12**, 637-647.

Meyers, M., Chen, P., Lin, A. and Seki, Y. (2008). Biological materials: structure and mechanical properties. *Prog. Mater. Sci.* **53**, 1-206.

Miller, L. M., Little, W., Schirmer, A., Sheik, F., Busa, B. and Judex, S. (2007). Accretion of bone quantity and quality in the developing mouse skeleton. *J. Bone Miner. Res.* **22**, 1037-1045.

Mollet, H. F. (2002). Distribution of the pelagic stingray, *Dasyatis violacea* (Bonaparte, 1832), off California, Central America, and worldwide. *Mar. Freshw. Res.* **53**, 525-530.

Moss, M. (1977). Skeletal tissues in sharks. *Am. Zool.* **17**, 335-342.

Porter, M. E., Beltrán, J. L., Koob, T. J. and Summers, A. P. (2006). Material properties and biochemical composition of mineralized vertebral cartilage in seven elasmobranch species (Chondrichthyes). *J. Exp. Biol.* **209**, 2920-2928.

Porter, M. E., Koob, T. J. and Summers, A. P. (2007). The contribution of mineral to the material properties of vertebral cartilage from the smooth-hound shark. *J. Exp. Biol.* **210**, 3319-3327.

Reilly, D. and Burstein, A. (1975). The elastic and ultimate properties of compact bone and tissue. *J. Biomech.* **8**, 393-405.

Reilly, D., Burstein, A. and Frankel, V. (1974). The elastic modulus for bone. *J. Biomech.* **7**, 271-275.

Roy, M. E., Nishimoto, S. K., Rho, J. Y., Bhattacharya, S. K., Lin, J. S. and Pharr, G. M. (2000). Correlations between osteocalcin content, degree of mineralization, and mechanical properties of *C. carpio* rib bone. *J. Biomed. Mater. Res.* **54**, 547-553.

Schaffler, M. B. and Burr, D. B. (1988). Stiffness of compact bone: effects of porosity and density. *J. Biomech.* **21**, 13-16.

Schriefer, J. L., Robling, A. G., Warden, J. W., Fournier, A. J., Mason, J. J. and Turner, C. H. (2005). A comparison of mechanical properties derived from multiple skeletal sites in mice. *J. Biomech.* **38**, 467-475.

Sedlin, E. D. (1965). A rheologic model for cortical bone – a study of physical properties of human femoral samples. *Acta Orthop. Scand.* **S83**, 1-77.

Spatz, H. C., O'Leary, E. J. and Vincent, J. F. V. (1996). Young's moduli and shear moduli in cortical bone. *Proc. R. Soc. Lond. B* **263**, 287-294.

Summers, A. P. (2000). Stiffening the stingray skeleton – an investigation of durophagy in myliobatid stingrays (Chondrichthyes, Batoidea, Myliobatidae). *J. Morphol.* **243**, 113-126.

Summers, A. P., Koob, T. J. and Brainerd, E. L. (1998). Stingray jaws strut their stuff. *Nature* **395**, 450-451.

Summers, A. P., Ketcham, R. A. and Rowe, T. (2004). Structure and function of the horn shark (*Heterodontus francisci*) cranium through ontogeny: development of a hard prey specialist. *J. Morphol.* **260**, 1-12.

Swartz, S. and Middleton, K. M. (2008). Biomechanics of the bat limb skeleton: scaling, material properties, and mechanics. *Cells Tissues Organs* **187**, 59-84.

Szarko, M., Muldrew, K. and Bertram, J. E. A. (2010). Freeze–thaw treatment effects on the dynamic mechanical properties of articular cartilage. *BMC Musculoskel. Disord.* **11**, 231-239.

Toppe, J., Albrektsen, S., Hope, B. and Aksnes, A. (2007). Chemical composition, mineral content and amino acid and lipid profiles in bones from various fish species. *Comp. Biochem. Physiol. B* **146**, 395-401.

Vogel, S. (2003). *Comparative Biomechanics: Life's Physical World*. Princeton, NJ: Princeton University Press.

Wainwright, S. A., Biggs, W. D., Currey, J. D. and Gosline, J. M. (1976). *Mechanical Design in Organisms*. Princeton, NJ: Princeton University Press.

Withers, P. C., Morrison, G., Hefter, G. T. and Tek-Siong, P. (1994). Role of urea in buoyancy of elasmobranchs. *J. Exp. Biol.* **188**, 175-189.

Woo, S., Kuei, S., Amiel, D., Gomez, M., Hayes, W., White, F. and Akeson, W. (1981). The effect of prolonged physical training on the properties of long bone – a study of Wolff's law. *J. Bone Joint Surg. Am.* **63**, 780-787.

Zioupos, P., Currey, J. D., Casinos, A. and Buffrénil, V. (1997). Mechanical properties of the rostrum of the whale *Mesoplodon densirostris*, a remarkably dense bony tissue. *J. Zool.* **241**, 725-773.

Zioupos, P., Currey, J. D. and Casinos, A. (2000). Exploring the effects of hypermineralisation in bone tissue by using an extreme biological example. *Conn. Tiss. Res.* **41**, 229-248.